Research Square

Preprints are preliminary reports that have not undergone peer review.
They should not be considered conclusive, used to inform clinical practice,
or referenced by the media as validated information.

Genotype-dependent physiological markers for embryogenic callus induction in Korean pine

Ying Duan
Qiqihar University
Yue Zhong
Qiqihar University
Kun Zhu
Qiqihar University
Lu Zhou
Qiqihar University
Ruhui Wang
Qiqihar University
Yan Liang
liangyanyanliang@126.com
Qiqihar University

Research Article

Keywords: Pinus koraiensis, Embryogenic callus induction, Genotype dependency, Physiological markers

Posted Date: November 13th, 2026

DOI: https://doi.org/10.21203/rs.3.rs-11442908/v1

License: This work is licensed under a Creative Commons Attribution 4.0 International License.
Read Full License

Additional Declarations: No competing interests reported.

Genotype-dependent physiological markers for embryogenic callus induction in Korean pine

Ying Duan [1†], Yue Zhong [1†], Kun Zhu [1, 2], Lu Zhou[1, 2], Ruhui Wang [1], Yan Liang [1, 2*]

[1] School of Life Sciences and A & F, Qiqihar University, Qiqihar, 161006, China
[2] Heilongjiang Provincial Key Laboratory of Resistance Gene Engineering and Protection of Biodiversity in Cold Areas, Qiqihar University, Qiqihar, 161006, China
* Correspondence: liangyanyanliang@126.com

Abstract: The application of the established somatic embryogenesis (SE) system of Korean pine (*Pinus koraiensis*) has been largely limited by strong genotype dependence in embryogenic callus (EC) induction. To identify genotype-dependent markers for screening responsive genotypes, we compared physiological traits of one sensitive Korean pine EC-producing genotype and two recalcitrant genotypes: one that produces low-embryogenic callus (LEC) and another that produces non-embryogenic callus (NEC). At the early stage of embryogenic competence acquisition, the EC genotype was characterized by higher indole-3-acetic acid (IAA), methyl jasmonate (MeJA), peroxidase (POD), and malondialdehyde (MDA), coupled with moderate hydrogen peroxide (H_2O_2), while exhibiting lower abscisic acid (ABA) and catalase (CAT). During subsequent callus expansion without subculture, the EC genotype maintained moderate H_2O_2, elevated POD and superoxide dismutase (SOD), coupled with a reduced IAA/zeatin-riboside (ZR) ratio and decreased MDA. In contrast, the LEC genotype had lower ZR but higher IAA/ABA, MeJA/ABA, gibberellins (GA_3)/ABA, brassinosteroids (BR)/ABA, and ZR/ABA ratios, with significantly reduced SOD, potentially explaining its late-stage loss of embryogenic competence. In summary, this study identifies stage-specific physiological indicators, including phytohormone profiles, redox homeostasis, and oxidative damage, for early Korean pine genotype screening. Critically, embryogenic competence hinges on a two-phase transition: from "hormone-triggered oxidative signaling" during initiation to "hormonal equilibrium coupled with antioxidative defense" during maintenance, whereas failure (hormonal imbalance plus low SOD) may lead to loss of embryogenic competence in LEC. These findings identify physiological markers for early screening of Korean pine genotypes and provide insights into reversible transition between somatic and embryogenic cell states.

Key message: Hormone homeostasis and redox physiology serve as critical indicators for identifying responsive genotypes capable of the two-phase cell state transition toward embryogenic competence in Korean pine.

Keywords: *Pinus koraiensis*; Embryogenic callus induction; Genotype dependency; Physiological markers

1. Introduction

Korean pine (*Pinus koraiensis*) is an ecologically and economically important coniferous species native to Northeast Asia, including China, South Korea, North Korea, Japan, and the Russian Far East. In China, it is particularly notable as a dominant species in the temperate broad-leaved Korean pine forests of Northeast China. Its timber and nutrient-rich seeds are highly valued for food, cosmetics, and pharmaceuticals. However, over-harvesting of timber and pine nuts has resulted in substantial decline in the natural populations of Korean pine (Liang et al. 2022). Given the genetic variation and low reproductive efficiency that undermine conventional propagation (Peng et al. 2020), there is an urgent need for reliable techniques to produce high-quality Korean pine seedlings to conserve resources and ensure sustainable supply. As such, efficient propagation techniques for Korean pine are important for both ecological restoration and large-scale forestry production. Among various clonal propagation methods, somatic embryogenesis (SE) technology is widely known as the fastest and most efficient approach to achieve mass production of superior clonal seedlings with elite traits, meeting the demand of conifer seedling production. Additionally, this technique can be employed in artificial seed production and genetic transformation, thus enabling the rapid multiplication of superior genotypes (Egertsdotter et al. 2019).

In general, SE pathways can be either direct or indirect. Indirect SE pathways are more common in conifers, where somatic cells undergo progressive dedifferentiation into embryogenic callus (EC), followed by somatic embryo formation (Valentina et al. 2021). For Korean pine, this indirect SE likewise depends on the formation of EC, making efficient EC induction a critical prerequisite for its successful SE. However, despite the successful establishment of a Korean pine SE regeneration system from immature zygotic embryos, the initial EC induction rates remain low and exhibit strong genotype dependence. For numerous recalcitrant genotypes, callus with high embryogenic potential cannot be induced even under optimized conditions, constituting a major bottleneck for research progress and commercial

deployment of this technology (Liang et al. 2025). Similarly, studies on *Pseudotsuga menziesii* (Walther et al. 2021), *Larix kaempferi* (Wang et al. 2022), and *L. principis-rupprechtii* (Chen et al. 2025) have demonstrated that the capacity for EC formation is strongly genotype-dependent. Additionally, investigations on *L. kaempferi* (Wang et al. 2022) and *P. menziesii* (Walther et al. 2021) revealed that different genotypes exhibit distinct responses to EC induction, yielding a mixture of EC and non-embryogenic callus (NEC) under identical culture conditions. Collectively, genotype dependence is a widespread phenomenon in plant SE, particularly in conifers following indirect SE pathways.

During plant SE, somatic cells undergo structural rearrangement, and their fate switch is widely recognized to depend on a coordinated cascade of morphological, physiological, and molecular changes that give rise to embryogenic cells *in vitro*. This transition, in turn, involves cell dedifferentiation and epigenetic reprogramming via specific signal transduction pathways to regain embryogenic potential. Afterwards, embryogenic cells further develop and differentiate into mature somatic embryos (Mcfarland and Kaeppler 2024). Notably, phytohormones act as central signaling molecules governing this sequence of cellular events. For instance, in *Brachypodium distachyon*, higher levels of indole-3-acetic acid (IAA) and gibberellins (GAs) promote the formation of mature embryo-produced compact EC , whereas higher trans-zeatin riboside (tZR) and lower abscisic acid (ABA) levels promote the development of immature embryo-produced compact EC, demonstrating the role of hormones in regulating the acquisition of embryogenic competence (Ouyang et al. 2026). In *Citrus reticulata*, EC were distinguished from NEC by multiple morphological and physiological traits, including denser cytoplasm, enlarged nuclei, abundant organelles, higher soluble proteins, increased activities of peroxidase (POD), superoxide dismutase (SOD), and catalase (CAT), and reduced reactive oxygen species (ROS) levels (Wang et al. 2026). These findings suggest that morphological and physiological markers can serve as effective tools for screening cells with embryogenic potential. Nevertheless, most studies deploy such markers only to classify calli as embryogenic or non-embryogenic post-induction, without addressing genotypic differences in the early events governing embryogenic competence acquisition. Accordingly, the underlying regulatory mechanisms have yet to be fully elucidated, particularly how oxidative stress, phytohormonal dynamics, and metabolic flux differ between genotypes during EC induction (Yue et al. 2022), as well as how genotype-dependent regulatory networks determine differential responses between sensitive and recalcitrant genotypes.

Consistent with Gao et al. (2021), our previous study revealed that different Korean pine genotypes exhibited varying responses to EC induction under identical culture conditions, producing calli with distinct embryogenic potentials, ranging from EC to low embryogenic callus (LEC) or NEC (Liang et al. 2025). In the present study, we systematically characterized the physiological traits of explants and derived calli from these genotypes during induction stages, aiming to identify markers that can predict the embryogenic potential of different genotypes prior to culture. Using these markers, we will be able to establish a more efficient EC induction system for Korean pine based on genotype, while offering insights into the reversible transition between somatic and embryogenic cell states.

2. Materials and Methods

2.1. Preparation of biological materials

Green immature female cones of three genotypes, including W135, W154, and L22-2, were collected from three open-pollinated (OP) trees growing in the Qingshan Korean pine seed orchard of Heilongjiang Province (W135, W154) and the Lushuihe Korean pine seed orchard of Jilin Province (L22-2), Northeastern China, from July 5 to 10 in 2024. Well-developed Korean pine seeds at the cleavage polyembryony stage were selected for this experiment. The developmental stages of zygotic embryos were examined before inoculation under a stereomicroscope (Olympus SZX 7). After removing the seed coat, the seeds were soaked in detergent for 30 min and then washed with running water for about 2 h. The explants were immersed in 75 % (v/v) ethanol for 1-2 min, rinsed with sterile water 3-5 times, and immersed in 10 % NaClO (v/v) solution for 15 min, followed by three rinses in sterile water. Durzan medium (DCR) (Gupta and Durzan 1985) was used as the EC initiation medium, containing 6-benzyl adenine (6-BA; 1.5 mg • L^{-1}), 1-Naphthaleneacetic acid (NAA; 3 mg • L^{-1}), casein hydrolysate (0.5 g • L^{-1}), L-glutamine (0.5 g • L^{-1}), sucrose (30 g • L^{-1}), and phytagel (4 g • L^{-1}), with pH being adjusted to 5.8 before sterilization. The cultures were maintained for 30 d in the dark at 24 ± 2 ℃. Three replicates were employed per genotype, each consisting of 30 seeds randomly collected from the same cones. After 20 days of culture, the callus induction rate was calculated for each genotype.

$$\text{Callus induction rate (\%)} = \frac{\text{number of calli produced}}{\text{number of inoculated explants}} \times 100\%$$

2.2. Morphological observation

The morphological characteristics of the cultured explants, including induced callus at 5 d, 10 d, 15 d, 20 d, were observed under a stereomicroscope (Olympus, SZX7). Moreover, fresh callus at 5 d, 10 d, 15 d, and 20 d were randomly collected and stained with 1 % magenta acetate and 0.05 % evans blue (Filonova et al. 2000), and then these slides were observed and photographed under a light microscope (Olympus, BX51).

2.3 Determinations of physiological indices

The explants, including callus collected at 5 d, 10 d, 15 d and 20 d, were stored at -80 ℃ after rapid freezing in liquid nitrogen for the detection of physiological indexes. Each sample consisted of three biological replicates.

2.3.1 Endogenous hormones

Measurement of the endogenous hormones of different genotypes in Korean pine was performed using the ELISA kit (Demirkol and Yılmaz 2023). We measured the absorbance at 490 nm and determined the concentrations of IAA, zeatin-riboside (ZR), GA_3, ABA, brassinosteroids (BR), and methyl jasmonate (MeJA) using a standard curve.

2.3.2 Soluble protein content

Soluble protein content was analyzed according to the methods described by Peng et al. (2020), with minor modifications. Approximately 0.5 g of sample was homogenized in 5 mL pre-cooled phosphate buffer solution (pH 7.8). The homogenate was centrifuged at 1,0000 × g for 10 min at 4 ℃, and 0.1 mL of the supernatant was added to 5 mL of Coomassie brilliant blue G-250 solution (0.1 $g \cdot L^{-1}$). After 2 min, the soluble protein content was determined by measuring absorption at a wavelength of 595 nm.

2.3.3 Soluble sugar content

Soluble sugar content was determined using the anthrone method according to Peng et al. (2020) with minor modifications. Briefly, 0.5 g of sample was ground in liquid nitrogen and then mixed with 5 mL of 80 % ethanol. The mixture was boiled in a water bath at 80 ℃ for 30 min, followed by centrifugation at 12,000 × g for 15 min. Subsequently, 1 mL of the supernatant was collected and mixed with 5 mL of anthrone reagent. After boiling for 10 min, the absorbance was measured at 625 nm using a spectrophotometer.

2.3.4 Starch content

The method for extracting starch was modified according to Peng et al. (2020). Briefly, 2 mL of 9.2 M perchloric acid ($HClO_4$) was added to the pellet remaining after soluble carbohydrate extraction. The mixture was thoroughly stirred for 15 min and centrifuged at 10000 × g for 10 min at 4 ℃ to collect the supernatant. The precipitate was resuspended in 2 mL of 4.6 M $HClO_4$, stirred for another 15 min, and centrifuged under the same conditions. The two supernatants were combined and diluted to a final volume of 50 mL with double distilled water (ddH_2O). For colorimetric assay, 2 mL of the diluted extract was mixed with 5 mL of 0.1% (w/v) anthrone reagent, then incubated in a boiling water bath at 100 ℃ for 10 min. After rapid cooling to room temperature, the absorbance was measured at 620 nm. Starch concentration was calculated using a glucose standard curve, with a conversion factor of 0.9 to adjust for the mass difference between glucose and starch.

2.3.5 SOD activity

SOD activity was assayed by the nitroblue tetrazolium (NBT) photochemical reduction method with minor modifications according to Jariteh et al. (2015). Specifically, 0.5 g of sample was homogenized in 5 mL of 0.1 M sodium phosphate buffer (pH 7.8), and 5 mL of the extract was centrifuged at 4 ℃ and 12,000 × g for 15 min. The resultant supernatant was collected as crude SOD extract. Then, 3 mL reaction mixture (composed of 0.2 M sodium phosphate buffer (pH 7.8), 13 mM L-methionine, 75 μM NBT, 0.1 mM EDTA, and 75 mM riboflavin) was combined with the supernatant. The mixture was incubated at 25 ℃ in the dark for 15 min, and absorbance was subsequently determined at 560 nm.

2.3.6 CAT activity

For CAT activity assay, the method described by Huang et al. (2023) was adopted with slight modifications. The reaction mixture (50 mM PBS containing 0.1 mM EDTA, pH 7.8) was preincubated in a 25 ℃ water bath for 5 min prior to mixing with the enzyme extract. The reaction was initiated by the addition of 19 mM H_2O_2, and the change in absorbance at 240 nm was monitored over time.

2.3.7 POD activity

POD activity was evaluated using the method described by Jariteh et al. (2015) with minor modifications. Specifically, 0.5 g of sample was homogenized in 5 mL of 0.1 M sodium phosphate buffer (pH 7.8), and 5 mL of the extract was centrifuged at 4 ℃ and 12,000 × g for 15 min. The resultant supernatant was collected as crude SOD extract. Then,

3 mL reaction mixture (composed of 0.2 M acetate buffer (pH 4.8), 3% H_2O_2, and 20 mM benzidine) was combined with the supernatant. The mixture was incubated at 25 ℃ in the dark for 15 min, and absorbance was subsequently determined at 560 nm.

2.3.8 Malondialdehyde (MDA) content

MDA content was measured according to Jambunathan (2010) with minor modifications. Briefly, 0.8 g sample was homogenized in 0.1% trichloroacetic acid (TCA) solution. After centrifugation, the supernatant was mixed with TBA reagent. The mixture was heated, cooled, and subsequently centrifuged at 10,000 × g for 5 min at 4 ℃. The absorbance of the supernatant was measured at 532 nm.

2.3.9 Hydrogen peroxide (H_2O_2) content

H_2O_2 content was determined with the Hydrogen Peroxide Assay Kit (A064-1-1, Nanjing Jiancheng Bioengineering Institute, Nanjing, China). In short, 0.1 g sample was mechanically homogenized in 0.9 mL PBS (pH 7.0) in an ice-water bath. After centrifugation at 10,000 × g for 10 min, the supernatant was subjected to colorimetric measurement at 405 nm.

2.3.10 Statistical analysis of data

Statistical analyses were performed using SPSS v 21.0 (SPSS Inc., Chicago, IL, USA). Data were subjected to one-way analysis of variance (ANOVA), and mean comparisons were performed using Duncan's multiple range test at a significance level of $p < 0.05$. All values are expressed as the mean ± standard deviation (SD) from three independent biological replicates. Figures were prepared using Microsoft Excel 2024 and GraphPad Prism v 9.5 (GraphPad Software, USA).

3. Results

3.1. Influence of Korean pine genotypes on callus induction

In this study, female gametophyte explants at the cleavage polyembryony stage from three different Korean pine genotypes were used as explants to assess the effect of genotype on EC induction (Fig. 1A, a-c; f-h; k-m). After 20 days of culture, it was found that although numerically the callus induction rates were relatively close among the three genotypes, which were 39.08 % (L22-2), 29.44 % (W135), and 37.25 % (W154), respectively (Fig. 1B), there were obvious differences in external morphological and internal cytological characteristics of callus. Calli derived from genotype W135 were white, loose, and translucent (Fig. 1A, d). Notably, although this callus type was predominantly composed of large, irregular non-embryogenic cells (green circle), some small, regular embryogenic cells (red circle) were also observed (Fig. 1A, e). This type of callus turned brown after subculture with relatively low embryogenic potential and therefore, was designated as LEC. By contrast, W154-derived calli were white, opaque, compact, and granular (Fig. 1A, i), consisting largely of irregular non-embryogenic cells, with few typical embryogenic cells whose observed features were consistent with NEC (Fig. 1A, j). Calli from L22-2, however, were white, translucent, soft, and viscous, with filamentous structures on the surface (Fig. 1A, n), consisting of small, uniform, nearly round, and tightly packed embryogenic cells (Fig. 1A, o). Unlike the other two callus types, which turned brown during subsequent somatic embryos maturation, L22-2-derived calli successfully differentiated into somatic embryos, confirming their high embryogenic potential. Collectively, these findings demonstrate that EC induction in Korean pine is genotype-dependent: L22-2 produced exclusively EC (sensitive genotype), W154 produced predominantly NEC with scarce embryogenic components; whereas W135 formed a substantial proportion of EC together with NEC. Based on their browning responses and poor embryogenic performance after subculture, W154 and W135 were classified as recalcitrant genotypes.

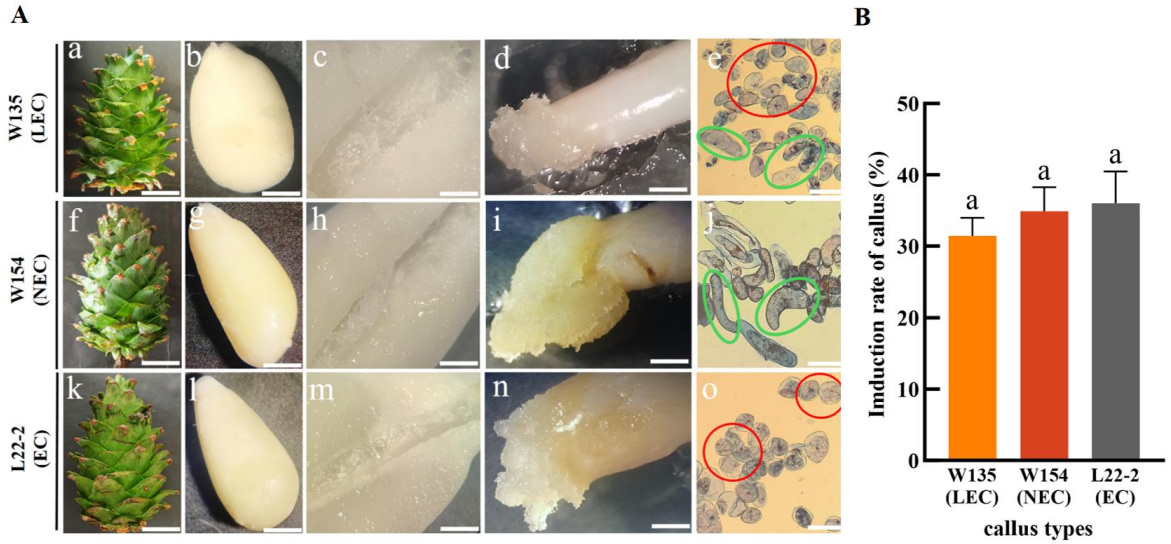


Fig 1. Cone, seeds, embryo development, callus morphology, histocytological observations and induction rates in different Korean pine genotypes

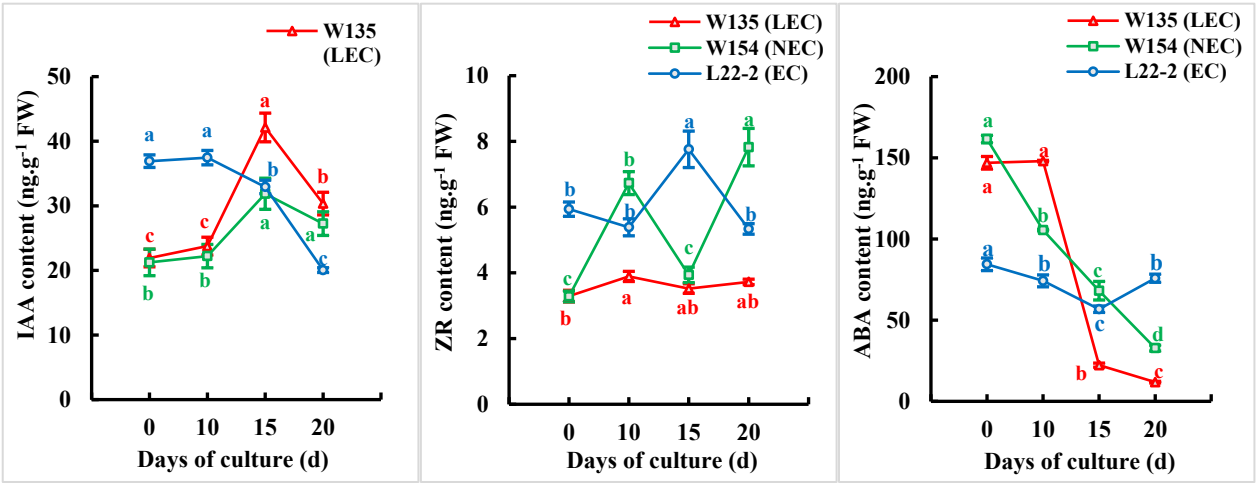
(A) Morphological observations of cones, seeds, embryonic developmental stages, callus, and histological sections of different Korean pine genotypes. a-e: Genotype W135; f-j: Genotype W154; k-o: Genotype L22-2. (a) Fresh cone of W135; (b) Seed of W135; (c) Cleavage polyembryony stage in a seed of W135; (d) LEC induced from W135; (e) Histological section of W135; (f) Fresh cone of W154; (g) Seed of W154; (h) Cleavage polyembryony stage in in a seed of W154; (i) NEC induced from W154; (j) Histological section of W154; (k) Fresh cone of L22-2; (l) Seed of L22-2; (m) Cleavage polyembryony stage in in a seed of L22-2; (n) EC induced from L22-2; (o) Histological section of L22-2. In panel e, the red circles indicate embryogenic cells, and the green circles indicate non-embryogenic cells. Scale bars: a, f, k = 40 mm; b, c, g, h, l, m = 2 mm; d, i, n = 0.5 mm; e, j, o = 1 mm.

(B) Callus induction rates of three callus types from different Korean pine genotypes.

3.2 The changes of endogenous hormones content and balance

3.2.1 Changes of endogenous hormones content

In contrast to the two recalcitrant genotypes, L22-2 maintained a high IAA content (36.92-37.46 ng • g^{-1} FW) from 0 to 10 days, followed by a continuous decline to a minimum of 20.05 ng • g^{-1} FW at day 20 ($p < 0.05$). In contrast, genotypes W135 and W154 remained relatively stable IAA during the first 10 days, and then IAA increased rapidly to peaks at 15 days (42.13 ng • g^{-1} FW for W135 and 31.87 ng • g^{-1} FW for W154). Thereafter, their trends diverged: IAA of W135 dropped back to its day 10 level by day 20 ($p < 0.05$), whereas W154 remained relatively stable IAA, ranging from 27.24 to 31.87 ng • g^{-1} FW during days 15-20 (Fig. 2).



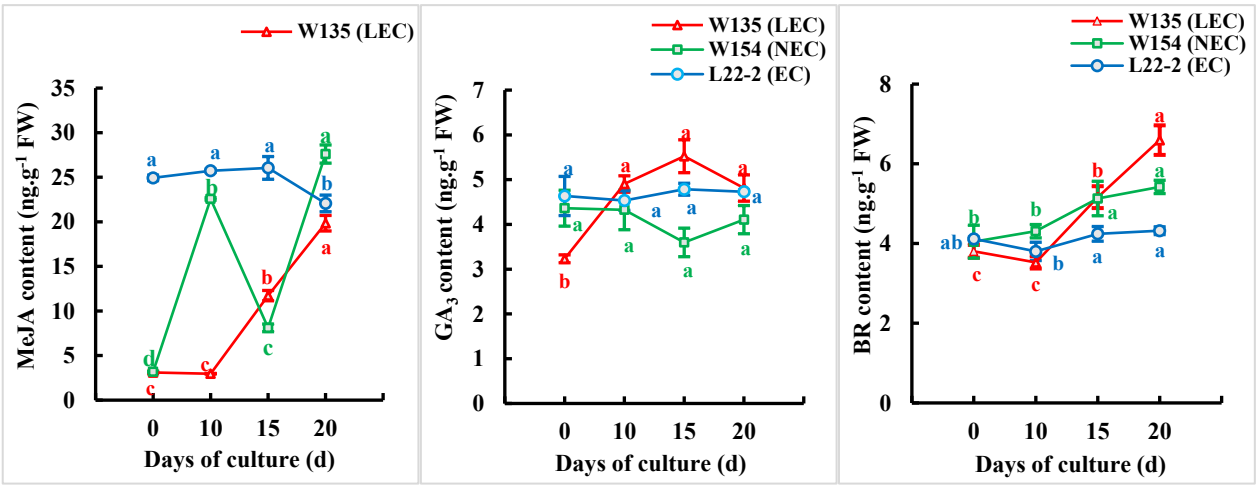


Fig 2. The changes in the content of endogenous hormones during the callus induction process of three Korean pine genotypes

The ZR content exhibited significantly different trends among the three Korean pine genotypes. For genotype L22-2, the ZR content remained relatively stable, high level from 0 to 10 days, being approximately twice that of genotypes W135 and W154 at day 0. Subsequently, a sharp increase in ZR content of L22-2 occurred between 10 and 15 days, peaking at 15 days (7.76 ng •g^{-1} FW), which was significantly higher than the levels at 5, 10, and 20 days ($p < 0.05$). In genotype W154, ZR content followed a fluctuating trend, increasing from days 5 to 10, decreasing between days 10 and 15, and then rising again from days 15 to 20. The lowest values were recorded at days 0 and 15 (3.28 and 3.94 ng • g^{-1} FW, respectively), while the highest value was observed at day 20 (7.83 ng • g^{-1} FW). In contrast to L22-2 and W154, genotype W135 maintained consistently low ZR levels throughout the experimental period (3.29-3.89 ng • g^{-1} FW), showing no significant changes over time ($p > 0.05$).

The three genotypes exhibited distinct ABA accumulation patterns. For W135, ABA levels remained high during the first 10 days (146.93 and 147.97 ng • g^{-1} FW at days 0 and 10, respectively), then decreased sharply to a minimum of 11.84 ng • g^{-1} FW at day 20, significantly lower than the levels at days 0, 10, and 15 ($p < 0.05$). In contrast, W154 showed a sustained decrease over the entire period, from 161.54 ng • g^{-1} FW at day 0 to 32.79 ng • g^{-1} FW at day 20. ABA of L22-2 decreased gradually from day 0 to day 15, reaching a minimum of 56.75 ng • g^{-1} FW at day 15, then recovered by day 20 to a level comparable to that at day 10 ($p < 0.05$). Notably, its initial ABA content at day 0 (84.41 ng • g^{-1} FW) was significantly lower than those of W135 and W154.

The MeJA content also showed markedly different dynamics across the three Korean pine genotypes. In genotype L22-2, MeJA levels moderately increased from day 0 to day 15 (24.93-26.05 ng • g^{-1} FW), followed by a sharp decline from day 15 to day 20, reaching the minimum value of 22.07 ng • g^{-1} FW at day 20, which was significantly lower than those detected in days 0-15 ($p < 0.05$). In comparison with L22-2, genotypes W135 and W154 exhibited relatively low MeJA levels at day 0 (3.10 and 3.18 ng • g^{-1} FW, respectively). MeJA contents in W154 followed an "increase-decrease-increase" pattern: its contents rose rapidly from days 0 to 10, declined sharply over days 10-15, and subsequently increased greatly from days 15 to 20. The minimum content (3.18 ng • g^{-1} FW) was detected at day 0, whereas the maximum value (27.61 ng • g^{-1} FW) appeared at day 20. For W135, MeJA content remained low from days 0 to 10 and increased gradually thereafter, peaking on day 20 (19.85 ng • g^{-1} FW), significantly higher than that at 0-15 d ($p < 0.05$).

GA_3 content showed no significant changes over the entire sampling period in both W154 and L22-2 ($p > 0.05$). In contrast, GA_3content in W135 was lowest at day 0 (3.23 ng • g^{-1} FW), which was significantly lower than the values observed from days 10 to 20 ($p < 0.05$). It increased sharply from day 0 to day 10, and then remained relatively stable at 4.81-5.52 ng • g^{-1} FW thereafter.

Similar to GA_3, BR content was low in all three genotypes (3.53-6.60 ng • g^{-1} FW). In W135 and W154, BR levels stayed low from days 0 to 10, ranging from 3.53 to 4.31 ng • g^{-1} FW. In W135, BR contents increased gradually during 10-20 d and reached its maximum (6.60 ng • g^{-1} FW) at day 20. In W154, BR contents increased from days 10 to 15 and remained stable thereafter from days 15 to 20. BR content of L22-2 decreased initially (days 0-10), followed by an increase (days 10-15), and gradually stabilized during days 15-20, reaching a minimum of 3.80 ng • g^{-1} FW on day 10.

In summary, to obtain calli with high embryogenic potential, initial explants of the sensitive Korean pine genotype required high levels of IAA, ZR and MeJA, together with a low level of ABA. During the subsequent callus expansion phase without subculture, elevated levels of ZR and MeJA, alongside low IAA, became critical factors. In contrast, for the two recalcitrant genotypes, the effects of individual hormones also varied.

3.2.2 Changes in the ratio of endogenous hormone content

As illustrated in Fig. 3, the IAA/ZR ratios (3.30-11.99) in all three genotypes were markedly higher than the ratios of IAA/ABA, MeJA/ABA, GA_3/ABA, BR/ABA, and ZR/ABA (all < 2.6).

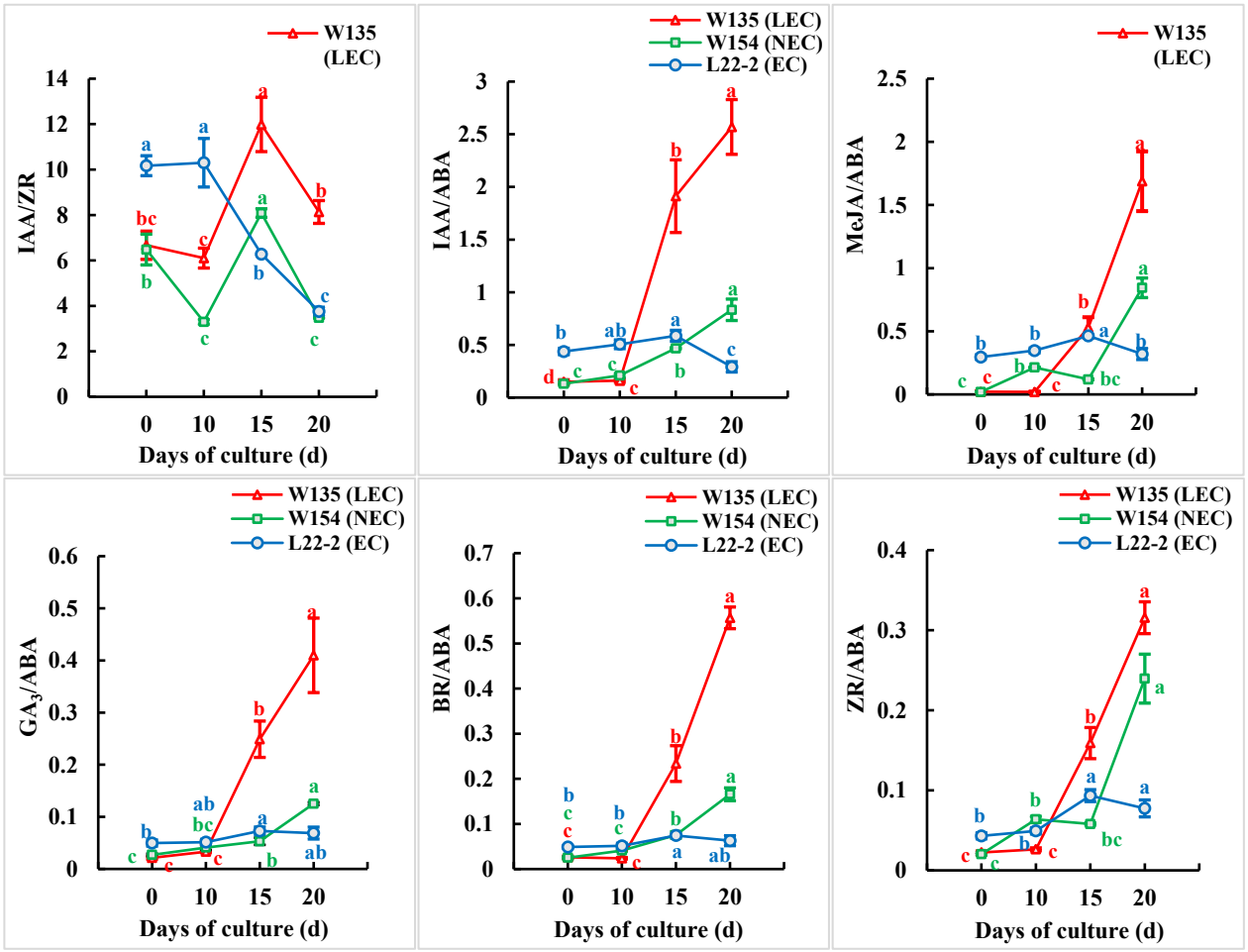


Fig 3. The changes in the ratio of endogenous hormones during the callus induction process of three Korean pine genotypes

Specifically, in L22-2, the value of IAA/ZR remained high from days 0 to 10 (10.17 and 10.30, respectively). It declined gradually after day 10 and reached its minimum at day 20 (3.76). Unlike L22-2, the ratio in W135 fluctuated slightly during 0-10 d, rising sharply from days 10 to 15, with the maximum value observed at day 15 (11.99), and subsequently decreasing to a low level at day 20 comparable to that at day 0 ($p < 0.05$). Similar to W135, the IAA/ZR ratio of W154 exhibited a "decrease-increase-decrease" trend, peaking at day 15 (8.08). Notably, the IAA/ZR ratios of W135 and W154 at day 0 were relatively low (6.67 and 6.48, respectively) compared with L22-2 (10.17).

Unlike the IAA/ZR ratio (6.11-6.67), the other five ratios (IAA/ABA, MeJA/ABA, GA_3/ABA, BR/ABA and ZR/ABA) in W135 remained relatively low (0.02-0.16) with minor fluctuations from days 0 to 10. These ratios rose sharply after day 10 and peaked at day 20, with the highest being 2.56 for IAA/ABA. For L22-2 and W154, these ratios remained low with mild fluctuations from days 0 to 15; however, W154 showed a substantial increase from days 15 to 20. In contrast, from days 10 to 15, the sensitive genotype L22-2 maintained stable ratios or increased slightly, and thereafter kept steady levels or increased moderately from days 15 to 20.

Thus, we found a high IAA/ZR ratio was observed in initial explants as well as in tissues undergoing early embryogenic competence acquisition, whereas a lower ratio more favorable during the subsequent callus expansion phase in the sensitive genotype. In contrast to the sensitive genotype, low IAA/ZR ratios were observed in the two

recalcitrant genotypes at the initial stages, which may favour early LEC and NEC formation. Furthermore, high ratios of IAA/ABA, MeJA/ABA, GA_3/ABA, BR/ABA and ZR/ABA may favour LEC formation during the middle and late stages.

3.3 Changes in stored substances and antioxidant indices

3.3.1 Changes of stored substances

Overall, as shown in Fig. 4, soluble protein contents showed no significant differences over time or among genotypes ($p < 0.05$), ranging from 0.14 to 0.15 mg • g^{-1} FW throughout the induction period.

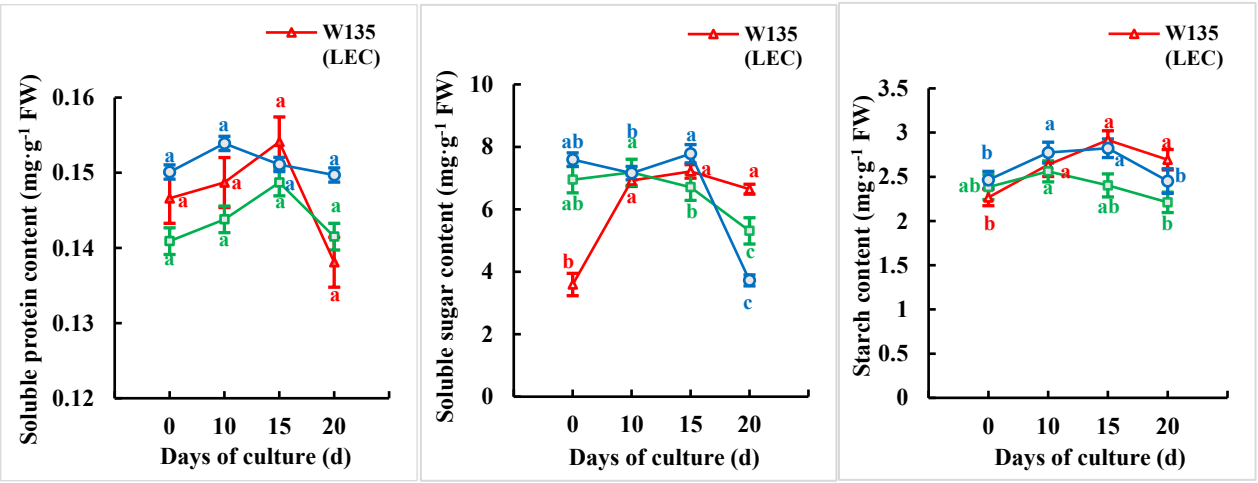


Fig 4. Changes of nutritional indexes during the callus induction process of three Korean pine genotypes

Specifically, in W154 and L22-2, soluble sugar contents kept stable or fluctuated slightly from days 0 to 15 before declining sharply by day 20. Minimum values occurred at day 20 (5.31 and 3.72 mg • g^{-1} FW, respectively for W154 and L22-2), significantly lower than their respective levels on days 0, 5 and 15 ($p < 0.05$). In comparison with the above two genotypes, W135 exhibited a lower soluble sugar content at day 0 (3.59 mg • g^{-1} FW), which was significantly lower than the values from days 5 to 20 ($p < 0.05$). The content rose sharply over days 0-10 and then remained stable from days 10 to 20 (6.64-7.21 mg • g^{-1} FW).

Consistent with the variation of soluble protein contents, starch contents varied slightly across the three Korean pine genotypes throughout the sampling period (2.21-2.92 mg • g^{-1} FW). W135 showed an initial increase in starch content from days 0 to 10, followed by a relatively stable stage from days 10 to 20. In L22-2, starch content increased (0-10 d), then remained relatively stable (10-15 d), and finally decreased (15-20 d), reaching a low level at day 20 comparable to that at day 0 ($p < 0.05$). Starch content in W154 only fluctuated slightly over 0-20 d (2.21-2.56 mg • g^{-1} FW) .

3.3.2 Changes of antioxidant indices

Compared with the two recalcitrant genotypes, the sensitive genotype exhibited higher MDA content during the first 10 days. Its levels remained stable from day 0 to day 10, and then decreased sharply between days 10 and 20, reaching a minimum of 0.82 μmol • g^{-1} FW at day 20. MDA content in W135 increased significantly from days 0 to 15 and then stayed stable from days 15 to 20. By contrast, MDA content in W154 remained relatively low and stable throughout the culture period, fluctuating from 0.63 to 0.77 μmol • g^{-1} FW. Notably, the two recalcitrant genotypes exhibited comparable MDA content (Fig. 5).

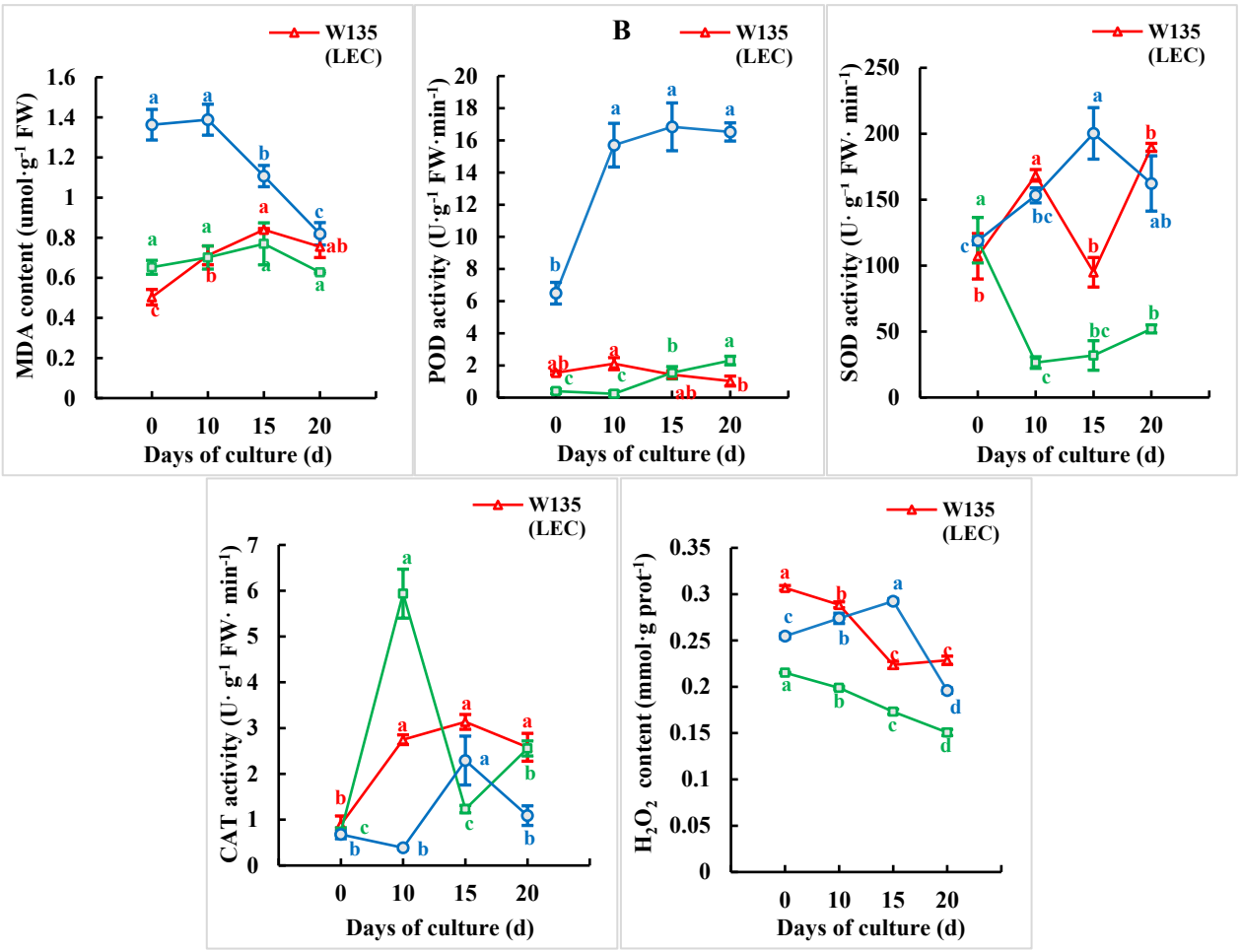


Fig 5. Changes of antioxidant indices during the callus induction process of three Korean pine genotypes

Compared to the two recalcitrant genotypes, the sensitive genotype exhibited higher POD activity (6.50-16.84 U •g^{-1} FW •min^{-1}), which increased dramatically from days 0 to 10 (6.50 and 15.70 U •g^{-1} FW •min^{-1} , respectively), with no significant changes observed from days 10 to 20 ($p < 0.05$). For the two recalcitrant genotypes, POD activity remained at a low level throughout 0-20 d (0.40-2.31 U •g^{-1} FW •min^{-1}). POD activity in W135 exhibited slight fluctuations throughout the period, while POD activity in W154 stayed stable between day 0 and day 10, increased gradually thereafter, and peaked on day 20 at 2.31 U • g^{-1} FW • min^{-1}.

SOD activity in the initial explants of the three Korean pine genotypes was comparable, ranging from 109.19 to 119.28 U • g^{-1} FW. However, as callus induction progressed, distinct genotype-dependent dynamic patterns emerged. Specifically, W154 sustained consistently low SOD activity during 10-20 d, corresponding to NEC formation. For L22-2, SOD activity increased progressively from day 0 to day 15, reaching a peak of 200.27 U •g^{-1} FW at day 15, before decreasing slightly by day 20; however, this decline was not statistically significant ($p > 0.05$). By contrast, W135 exhibited a biphasic SOD activity pattern, with peaks at day 10 (168.46 U • g^{-1} FW) and day 20 (189.69 U • g^{-1} FW) , interspersed with a pronounced trough on day 15. The two peak values were not significantly different ($p > 0.05$), yet both were markedly higher than the SOD activity levels observed on days 0 and 15 ($p < 0.05$).

CAT activity differed significantly among the three Korean pine genotypes, with minimal differences observed at 0 d. In L22-2, it was stable (0-10 d), increased (10-15 d), peaking at day 15 (2.29 U • g^{-1} FW • min^{-1}), which was significantly higher than those at days 0, 10, and 20 ($p < 0.05$). In W135, CAT activity increased from 0 to 10 d, with the minimum value detected at day 0 (0.89 2.29 U • g^{-1} FW • min^{-1}), and maintained a stable level between 10 and 20 d (2.58-3.14 U • g^{-1} FW • min^{-1}). Meanwhile, W154 followed an "up-down-up" trend, with a peak at day 10 (5.94 U • g^{-1} FW • min^{-1}).

In the sensitive genotype, H_2O_2 content increased gradually from day 0 to 15, reached a maximum at day 15 (0.29 mmol • g prot^{-1}), and then decreased between days 15 and 20. By contrast, in the two recalcitrant genotypes, H_2O_2

content decreased continuously throughout the process, with peak values at day 0 of 0.31 and 0.22 mmol • g prot^{-1}, respectively. Notably, the sensitive genotype exhibited an intermediate initial content at day 0 (0.26 mmol • g prot^{-1}) relative to the two recalcitrant genotypes.

4. Discussion

High-frequency EC induction is critical for establishing somatic embryogenesis (SE) systems in conifers, yet it remains challenging in Korean pine owing to low induction rates and strong genotype dependency (Liang et al. 2022). Although this challenge is widespread across conifer SE systems (Walther et al. 2021; Wang et al. 2022; Chen et al. 2025), the underlying regulatory mechanisms remain poorly understood (Zhang et al. 2024). Thus, reliable markers for screening responsive genotypes are urgently needed to predict EC competence at an early stage. To address this, we compared physiological indicators between sensitive and recalcitrant Korean pine genotypes to identify genotypes with high EC induction capacity. Furthermore, given that our previous study revealed a gradual transition from LEC to NEC in the recalcitrant genotype W135 during the late induction stages (Liang et al. 2025), the present study was also aimed to elucidate the physiological basis underlying this loss of embryogenic competence.

4.1. The role of endogenous hormones during EC induction in Korean pine genotypes with contrasting embryogenic potential

The acquisition of embryogenic competence in somatic cells is regulated by multiple physical and chemical factors, among which endogenous hormones are of paramount importance. Auxin and cytokinins (CTKs), in particular, are critical initiators for somatic cells to acquire embryogenic competence, modulating cell division and differentiation (Yue et al. 2022). In our study, the sensitive Korean pine genotype exhibited higher IAA levels in initial explants compared with two recalcitrant genotypes, whereas its IAA content remained low during the subsequent callus expansion phase without subculture, suggesting that IAA is essential for the somatic-to-embryogenic cell fate switch. This auxin requirement has been well documented in *Medicago truncatula* (Ewa and Anna 2021), *Solanum betaceum* (André et al. 2022), and *Passiflora edulis* (Lima et al. 2024), where higher IAA content was observed in initial explants of EC-induction versus NEC-forming explants, with a subsequent decline during EC formation. Collectively, these findings indicate that high IAA levels promote EC initiation in Korean pine, whereas low IAA levels are essential forvigorous EC growth and maintenance of high embryogenic potential.

Beyond the central function of auxin in driving somatic cell dedifferentiation and EC initiation, CTKs also participate in this reprogramming event. Nevertheless, CTKs do not function as stand-alone triggers; rather, they act synergistically with auxin to modulate this reprogramming process and facilitate the acquisition of embryogenic competence (Wang et al. 2021). In this study, the ZR content in the initial explants of the sensitive Korean pine genotype was significantly higher than that in the two recalcitrant genotypes, suggesting that high CTK levels are associated with the formation of embryogenic cells. This corroborates previous findings that high concentrations of exogenously supplied auxin and CTKs are required for EC induction (Kamble et al. 2024). It further suggests that differences in endogenous CTK abundance among Korean pine genotypes partly account for the formation of callus with divergent embryogenic competence.

Our results indicated that high MeJA levels in the explants favored EC induction in Korean pine. While the role of MeJA in SE has been rarely investigated, existing evidence suggests stage specific effects: our previous study demonstrated that MeJA promotes somatic embryo differentiation in this species (Liang et al. 2022), and a study on *Artemisia maritima* reported its beneficial impacts on somatic embryo maturation and germination (Nabi et al. 2025).

Furthermore, our results revealed that the sensitive Korean pine genotype exhibited significantly lower ABA levels than the recalcitrant genotypes during early EC induction, consistent with reports in *M. truncatula* demonstrating that low endogenous ABA favors EC formation (Ewa and Anna 2021).

In addition to the regulation of individual hormones, the acquisition of embryogenic competence during plant SE is governed by the intricate balance among multiple phytohormones (Liang et al. 2022). The IAA:CTK ratio, in particular, modulates cell polarity and cell reprogramming during cell differentiation and redifferentiation in most plant species (Chen et al. 2025). Consistent with these findings, our results demonstrate that auxin-cytokinin dynamics (represented by the IAA/ZR ratio in this study) are critical for the somatic-to-embryogenic cell transition in Korean pine. More specifically, a higher IAA/ZR ratio favored EC initiation in the sensitive Korean pine genotype, whereas a lower ratio was more conducive to the subsequent vigorous growth of EC. Moreover, during vigorous growth after LEC induction, we found that the ratios of IAA/ABA, MeJA/ABA, GA_3/ABA, BR/ABA, and ZR/ABA were all higher than those in NEC and EC during their respective induction. This unique hormonal signature indicates that LEC maintains a distinct hormonal homeostasis relative to EC and NEC at this identical post-induction stage, which poten-

tially contributes to the progressive loss of embryogenic competence in LEC. Overall, these findings indicate that differences in hormonal balance represent a key factor underlying genotypic differences in both the acquisition and subsequent maintenance of embryogenic competence in Korean pine. Additionally, given that callus status depends heavily on both exogenous hormone application and endogenous hormonal balance (Lu et al. 2020), our findings can be used not only to screen responsive genotypes but also to optimize hormone treatment regimes.

4.2 The role of stored substances during EC induction in Korean pine genotypes with contrasting embryogenic potential

Besides endogenous hormones, embryogenic culture initiation depends on multiple factors including storage substances (proteins, starch and soluble sugars) (Peng et al. 2020). These metabolites synergistically provide energy for the somatic-to-embryogenic cell transition, EC proliferation and somatic embryo differentiation during SE (Pernis et al. 2026). In this study, soluble proteins showed no significant differences over time or among genotypes, and starch varied only within a narrow range without a consistent genotypic pattern. Soluble sugars, however, differed among genotypes: the LEC-producing genotype was markedly lower than the EC- and NEC-producing genotypes at day 0, then rose rapidly to reach levels comparable to both by days 10-15; yet from days 15-20, sugar levels declined in the EC- and NEC-producing genotypes but remained high only in the LEC-producing genotype. This pattern, whereby soluble sugar levels were lowest initially, converged at mid-induction, and were uniquely sustained in LEC at late stages, indicates that soluble sugar levels neither changed monotonically with callus type nor remained stable over time. This dynamic feature may not serve as a robust indicator for discriminating among genotypes that produce EC, LEC, or NEC. Overall, none of these three storage substances exhibited a consistent genotype associated pattern of variation, and they may be insufficient on their own to account for the genotypic differences in EC induction. Unlike in *Hevea brasiliensis* (Gu et al. 2025), none of them appears likely to act as a primary determinant of genotype dependent EC induction in Korean pine, and their exact roles still require further functional validation.

4.3 Oxidative stress responses during EC induction in Korean pine genotypes with contrasting embryogenic potential

Antioxidant enzymes such as SOD, CAT, and POD participate in ROS metabolism by regulating the homeostasis between superoxide ($O_2^{\cdot-}$) and H_2O_2, thereby supporting plant SE (Orłowska and Kępczyńska 2020). In this context, ROS levels are critical: moderate ROS levels promote dedifferentiation and differentiation, whereas excessive ROS triggers the loss of totipotency and cell death. Since the activities of these enzymes change dynamically alongside ROS levels during SE, they may serve as useful markers of SE progression (Przybył et al. 2024). Among these enzymes, POD is a potential biochemical marker for the early evaluation of embryogenic potential in callus (Sara et al. 2021). In our study, POD activity was significantly higher in the sensitive Korean pine genotype than in recalcitrant ones, consistent with the findings in *Ormosia henryi* (Wu et al. 2020), where elevated POD activity promoted embryogenic cell initiation and maintenance of the embryogenic state. This highlights POD's key role in embryogenic cell formation and embryogenic competence maintenance in Korean pine.

SOD initiates the antioxidant cascade by converting $O_2^{\cdot-}$ to O_2 and H_2O_2, playing a key role in redox homeostasis (Csongor et al. 2023). In Korean pine, initial SOD activity was comparable across genotypes, but its dynamics diverged during callus induction in a genotype-dependent manner. W154 exhibited persistently low SOD activity throughout 10-20 d, implying a possible association between NEC formation and reduced antioxidant capacity. Furthermore, SOD activity in the sensitive genotype exhibited a single peak at day 15, whereas the LEC-forming genotype exhibited a two-peak pattern. This suggests that the loss of embryogenic competence in LEC-forming genotypes may result from the absence of temporally coordinated SOD activation, implying that dynamic regulation of SOD activity may be required to maintain embryogenic competence. Likewise, Ren et al. (2022) reported an association between altered dynamic profiles of SOD activity and impaired embryogenic competence during EC subculture.

Consistent with the view that moderate oxidative stress facilitates embryogenic cell formation (Zhou et al. 2016), our study revealed higher MDA levels in the sensitive Korean pine genotype relative to the two recalcitrant genotypes during embryogenic cell initiation. Nevertheless, during further EC growth, MDA levels of the sensitive genotype declined markedly. Despite distinct MDA patterns between the two recalcitrant genotypes, the gap in MDA content between sensitive and recalcitrant genotypes gradually narrowed. These findings imply that reduced MDA accumulation contributes to maintaining embryogenic competence, as also reported previously (Nie et al. 2024).

CAT functions subsequent to SOD, decomposing H_2O_2 produced by SOD into H_2O and O_2, playing an essential role in mitigating oxidative stress (Csongor et al. 2023). In our study, CAT activity in the initial explants was low, with only minor differences among genotypes. In the LEC-forming genotype, CAT rose sharply within the first 10 days and

remained consistently high. Notably, our earlier work demonstrated that embryogenic competence was lost at day 15 in this genotype (Liang et al. 2025). Since this sustained high CAT activity precedes the loss of embryogenic competence, it may be linked to the decline in embryogenic potential in this genotype. In contrast, EC-forming sensitive genotype maintained stable CAT activity from 0 to 10 d, followed by a transient CAT peak at day 15 coinciding with maximum H_2O_2. This suggests that elevated CAT activity represents a defensive response against oxidative damage to support subsequent EC growth, rather than acting as a trigger for EC initiation. Another recalcitrant NEC forming genotype, W154, displayed a unique "up-down-up" CAT pattern peaking at day 10. Although its H_2O_2 levels also declined continuously, resembling the profile observed in the LEC forming genotype, W154 exhibited distinct CAT dynamics. Collectively, these CAT dynamics generate distinct H_2O_2 profiles. In the sensitive genotype, H_2O_2 accumulated gradually up to day 15 to maintain moderate ROS levels that support EC formation and subsequent growth. By contrast, both recalcitrant genotypes displayed continuously declining H_2O_2 levels, but diverged in regenerative performance: one gave rise to LEC that eventually converted into NEC, whereas W154 directly formed NEC and exhibited a distinct CAT temporal pattern. This aligns with the concentration dependent function of ROS, whereby moderate ROS levels facilitate the acquisition of embryogenic competence, whereas excessive ROS trigger cell death (Orłowska and Kępczyńska 2020). Nevertheless,genotypic variation likely underpins these differences in antioxidant associated physiological responses (Chen et al. 2026). Thus, the transient CAT peak in the sensitive genotype supported subsequent EC growth, whereas the sustained elevation in LEC-forming genotypes was associated with persistent stress and and the eventual loss of embryogenic competence. This highlights that temporal CAT dynamics, rather than absolute CAT levels, differentiate these two cell fates.

In summary, our quantitative analysis demonstrates that physiological homeostasis governs both the initiation and maintenance of embryogenic competence during EC induction in Korean pine. The acquisition of embryogenic competence is characterized by an oxidative burst (high POD, MDA, and H_2O_2; low CAT activity), accompanied by elevated IAA and MeJA levels and reduced ABA levels. Together, these factors prime the somatic-to-embryogenic transition. In contrast, EC growth and maintenance of high embryogenic potential require CTK dominant signalling (high ZR), a decreased IAA/ZR ratio, diminished MDA content, and sustained H_2O_2 acting as a potential signalling molecule. Notably, the LEC-forming genotype diverged from its NEC-producing counterpart during subsequent growth following callus induction, it exhibited lower ZR, persistently higher IAA/ABA, MeJA/ABA, GA_3/ABA, BR/ABA and ZR/ABA ratios, and significantly reduced SOD activity at day 15. Such hormonal-redox imbalance may disrupt the homeostasis required for the maintenance of embryogenic competence, ultimately causing loss of this capacity in this genotype. The LEC-forming genotype retained partial initial embryogenic competence, as reflected by its ability to activate CAT. Nevertheless, it could not maintain this capacity over time. This phenotypic defect may stem from an incomplete antioxidant network: although CAT became persistently elevated during 10-20 d, SOD returned to low levels at day 15, while POD and MDA remained at basal levels. This asynchronous activation, lacking functional integration, caused progressive oxidative damage and gradually depleted the initial embryogenic potential of LEC. By comparison, the NEC-forming genotype could not establish this partial coordinated antioxidant response, and its antioxidant system lacked the capacity for such sequential activation from the outset. Thus, the distinction between LEC and NEC may lie not solely in the presence or absence of embryogenic competence at the initial stage, but in the sustainability of that capacity-a sustainability that may depend on the completeness and temporal coordination of the antioxidant network.

These findings provide a physiological basis to interpret genotype-dependent differences in the initiation and maintenance of embryogenic competence during EC induction in Korean pine. Nevertheless, the regulatory networks underlying this hormonal-redox interplay, together with the contributions of dynamic changes in stored substances, remain to be fully elucidated. Future work combining integrated omics approaches and functional validation will help uncover key molecular targets, and thereby convert our current physiological findings into optimized culture protocols for recalcitrant Korean pine genotypes.

5. Conclusions

In this study, we profiled dynamic changes in endogenous hormones, storage substances and antioxidant systems during formation of three embryogenically distinct callus types (EC, LEC, NEC) from sensitive and recalcitrant Korean pine genotypes, and identified genotype-dependent physiological markers. The LEC-forming genotype showed early morphogenetic activation yet lost embryogenic capacity due to incomplete antioxidant networks and hormonal redox imbalance, whereas the NEC-forming genotype failed to trigger even partial activation of these pathways. These con-

trasting fates delineate the physiological thresholds that distinguish truly embryogenic from non- or transiently-competent callus. Notably, this physiological marker set may help identify genotypes with high embryogenic potential at callus initiation, avoiding the long waiting period for somatic embryo differentiation and facilitating the optimization of embryogenic callus induction conditions. Collectively, our work provides a physiological framework for embryogenic fate determination: bidirectional transitions between somatic and embryogenic cells in Korean pine are genotype-dependent. Genotypes modulate crosstalk among hormonal signals, redox homeostasis, and storage metabolites to govern embryogenic fate.

Author Contributions: Y.L. conceptualized and designed the study, provided technical guidance, and revised the manuscript. Y.D. drafted the original manuscript and assisted with data analysis. Y.Z. performed the majority of the experiments. Y.D. and Y.Z. contributed equally to this work. K.Z. and L.Z. contributed to data analysis and participated in constructive discussions. R.H.W. proofread the manuscript. All authors contributed to the experiments, revised the manuscript, and approved the final version of the manuscript.

Funding: This research was supported by the Natural Science Foundation of Heilongjiang Province (Grant No. PL2025C099), the Fundamental Research Funds for the Provincial Universities of Heilongjiang (Grant No. 145509230), and the Heilongjiang Provincial Undergraduate Training Program for Innovation and Entrepreneurship (Grant No. S202610232078).

Acknowledgments: We thank the support of the Qingshan Korean pine seed orchard of Heilongjiang Province and Lushuihe Korean pine seed orchard of Jilin Province for sample collection.

Compliance with ethical standards: The authors have no conflict of interest to report.

References

André C, Sandra C, Sandra C, Jorge C (2022) Induction of somatic embryogenesis in tamarillo (*Solanum betaceum* cav.) involves increases in the endogenous auxin indole-3-acetic acid. Plants. 11(10):1347. https://doi.org/10.3390/plants11101347

Chen SG, Gao F, Cao X, Dong HY, Zhan YC, Zhu LH, Tao J (2026) Roles of reactive oxygen species, storage compounds, and endogenous hormones in regulating somatic embryogenesis in blue spruce (*Picea pungens* Engelm.). Front Plant Sci. 16: 1646777. https://doi.org/10.3389/fpls.2025.1646777

Chen XY, Zhang LY, Liu CB, Wang R, Dai JF, Kong LS, Zhang JF, Zhao J (2025) The transcription factor Lpwrky65 enhances embryogenic capacity through reactive oxygen species scavenging during somatic embryogenesis of larch. Plant Physiol. 198(3). https://doi.org/10.1093/plphys/kiaf286

Csongor F, Tamás G, Zoltán K, Márta MH, Balázs TV, Petra JG, László UN, Adrienn K, Gábor V, Csaba M (2023) B and C subunits of *pp2a* regulate the levels of reactive oxygen species and superoxide dismutase activities in arabidopsis. Plant Physiol Biochem. 195:182-192. https://doi.org/10.1016/j.Plaphy.2022.12.031

Demirkol G, Yılmaz N (2023) Morphologically and genetically diverse forage pea (*Pisum sativum* var. *Arvense* L.) genotypes under single and combined salt and drought stresses. Plant Physiol Biochem. 196:880-892. https://doi.org/10.1016/j.plaphy.2023.02.041

Egertsdotter U, Ahmad I, Clapham D (2019) Automation and scale up of somatic embryogenesis for commercial plant production, with emphasis on conifers. Front Plant Sci. 10:109. https://doi.org/10.3389/fpls.2019.00109

Ewa K, Anna O (2021) Profiles of endogenous ABA, bioactive GAs, IAA and their metabolites in *Medicago truncatula* Gaertn. Non-embryogenic and embryogenic tissues during induction phase in relation to somatic embryo formation. Planta. 253(3): 67-67. https://doi.org/10.1007/s00425-021-03582-8

Filonova LH, Bozhkov PV, Von Arnold S (2000) Developmental pathway of somatic embryogenesis in *Picea abies* as revealed by time-lapse tracking. J Exp Bot. 51(343):249-264. https://doi.org/10.1093/jexbot/51.343.249

Gao F, Peng CX, Wang H, Shen HL, Yang L (2021) Selection of culture conditions for callus induction and proliferation by somatic embryogenesis of *Pinus koraiensis*. J For Res. 32(2):483-491. https://doi.org/10.1007/s11676-020-01147-1

Gu XC, Ao JY, Kong LS, Dai XM, Huang HS, Du HB, Wang XY, Huang TD (2025) Effects of explant source and orientation on secondary somatic embryogenesis in *Hevea brasiliensis*. Plants. 14(21):3274. https://doi.org/10.3390/PLANTS14213274

Gupta PK, Durzan DJ (1985) Shoot multiplication from mature trees of douglas-fir (*Pseudotsuga menziesii*) and sugar pine (*Pinus lambertiana*). Plant Cell Rep. 4: 177-179. https://doi.org/10.1007/BF00269282

Huang LJ, Ding LL, Wang WJ, Zhao LL, Zhao X, Wang PC (2023) Effects of simulated drought stress on the growth and physiological and biochemical parameters of *Paspalum wettsteinii*. Acta Physiol Plant. 45(6): 82. https://doi.org/10.1007/s11738-023-03556-1

Jambunathan N (2010) Determination and detection of reactive oxygen species (ROS), lipid peroxidation and electrolyte leakage

in plants. Methods Mol Biol (Clifton, N.J.). 639:292-298. https://doi.org/10.1007/978-1-60761-702-0_18

Jariteh M, Ebrahimzadeh H, Niknam V, Mirmasoumi M, Vahdati K (2015) Developmental changes of protein, proline and some antioxidant enzymes activities in somatic and zygotic embryos of persian walnut (*Juglans regia* L.). Plant Cell Tiss Organ Cult. 122(1):101-115. https://doi.org/10.1007/s11240-015-0753-z

Kamble VV, Rather SA, Razaq M, Phukela B, Gaikwad NB (2024) Elicitation of callus cultures of the medicinally important plant Embelia ribes Burm f. Using biotic and abiotic elicitors for enhanced production of embelin. Plant Cell Tiss Organ Cult. 159(1):14. https://doi.org/10.1007/s11240-024-02858-7

Liang Y, Li JH, Xu X, Yang QZ, Gao ML, Chen Y, Guan CY (2025) Genotype-dependent induction of embryogenic callus and programmed cell death in Korean pine. BMC Plant Biol. 25(1):910. https://doi.org/10.1186/s12870-025-06787-1

Liang Y, Xu X, Shen HL, Gao ML, Zhao Y, Bai X (2022) Morphological and endogenous phytohormone changes during long-term embryogenic cultures in Korean pine. Plant Cell Tiss Organ Cult.151(2):253-264. https://doi.org/10.1007/s11240-022-02348-8

Lima D, Simões S, Melo V, Mariana M, Adriano N, Coelho K, Coelho d, Lemes d, Campos O, Ismael R (2024) The dynamics of sugars, hormones, and cell wall epitopes dictate early somatic embryogenesis in passion fruit (*Passiflora edulis* Sims). Plant Cell Tiss Organ Cult. 157(1). https://doi.org/10.1007/s11240-024-02733-5

Lu H, Xu P, Hu KN, Xiao Q, Wen J, Yi B, Ma CZ, Tu JX, Fu TD, Shen JX (2020) Transcriptome profiling reveals cytokinin promoted callus regeneration in *Brassica juncea*. Plant Cell Tiss Organ Cult. 141(1):191-206. https://doi.org/10.1007/s11240-020-01779-5

Mcfarland LF, Kaeppler FH (2024) History and current status of embryogenic culture-based tissue culture, transformation and gene editing of maize (*Zea mays* L.). Plant Genome. 18(1):e20451. https://doi.org/10.1002/TPG2.20451

Nabi N, Singh S, Saffeullah P (2025) Methyl jasmonate elicitation improved growth, antioxidant enzymes, and artemisinin content in *in vitro* callus cultures of *Artemisia maritima* L. S Afr J Bot. 177:729-741. https://doi.org/10.1016/j.sajb.2025.01.001

Nie S, Yan Y, Wang Y, Liu SS, Guo WH, Yang L, Shen HL (2024) Proper doses of brassinolide enhance somatic embryogenesis in different competent Korean pine cell lines during embryogenic callus differentiation. Front Plant Sci. 15:1330103. https://doi.org/10.3389/fpls.2024.1330103

Orłowska A, Kępczyńska E (2020) Oxidative status in *Medicago truncatula* Gaertn. Non-embryogenic and embryogenic tissues with particular reference to somatic embryogenesis. Plant Cell Tiss Organ Cult. 140(1):35-48. https://doi.org/10.1007/s11240-019-01709-0

Ouyang D, Miao Y, Wei J, Ran L, Liu P, Xiong F, Yu X (2026) Plant hormones determine the differentiation of callus tissue during tissue culture of mature and immature *Brachypodium distachyon* embryos. Acta Physiol Plant.48(40). https://doi.org/10.1007/s11738-026-03910-z

Peng CX, Gao F, Wang H, Shen HL, Yang L (2020) Physiological and biochemical traits in Korean pine somatic embryogenesis. Forests. 11(5):577. https://doi.org/10.3390/f11050577

Pernis M, Mravec J, Klubicová K (2026) Starch dynamics as an important factor in early stages of somatic embryogenesis-a review. Front Plant Sci. 17:1832558. https://doi.org/10.3389/FPLS.2026.1832558

Przybył TH, Obarska A, Konecka A, Oberc JK, Wawrzyniak MK, Niczyporuk PA, Staszak AM, Ratajczak E (2024) Modulating ascorbic acid levels to optimize somatic embryogenesis in *Picea abies* (L.) h. Karst. Insights into oxidative stress and endogenous phytohormones regulation. Front Plant Sci. 15:1372764. https://doi.org/10.3389/FPLS.2024.1372764

Ren YH, Yu XQ, Xing JX, Tretyakova IN, Nosov AM, Yang L, Shen HL (2022) Interaction of subculture cycle, hormone ratio, and carbon source regulates embryonic differentiation of somatic cells in *Pinus koraiensis*. Forests. 13(10):1557. https://doi.org/10.3390/f13101557

Sara O, Kaoutar K, Mohammed B, Ilham B, Kenza L (2021) Peroxidase enzyme fractions as markers of somatic embryogenesis capacities in olive (*Olea europaea* L.). Plants. 10(5):901. https://doi.org/10.3390/plants10050901

Valentina PD, Daniela PF, Marcela DL, Felipe A, Erazzú LE (2021) Optimized somatic embryogenesis and plant regeneration in elite Argentinian sugarcane (*Saccharum* spp.) cultivars. J Genet Eng Biotechn. 19(1):171. https://doi.org/10.1186/s43141-021-00270-8

Walther M, Wagner I, Raschke J, Zoglauer K, Rupps A (2021) Abscisic acid induces somatic embryogenesis and enables the capture of high-value genotypes in douglas fir (*Pseudotsuga menziesii* [mirb.] franco). Plant Cell Tiss Organ Cult. 148(1): 45-59. https://doi.org/10.1007/s11240-021-02159-3

Wang JC, Zhang LF, Qi LW, Zhang SG (2022) Integrated transcriptomic and metabolic analyses provide insights into the maintenance of embryogenic potential and the biosynthesis of phenolic acids and flavonoids involving transcription factors in *Larix kaempferi* (Lamb.) carr. Front Plant Sci. 13:1056930. https://doi.org/10.3389/fpls.2022.1056930

Wang L, Miao XC, Zang XL, Cao ZZ, Hu LA, Sheng Y, Jiang LJ, Xu XY (2026) Comparative analysis of callus exhibiting differential somatic embryogenic potential and differentiation ability in *Citrus reticulata* Blanco reveals the regulatory role of *CrWOX11* in embryogenesis. Plant Cell Tiss Organ Cult. 164(1):21. https://doi.org/10.1007/s11240-025-03330-w

Wang YL, He SJ, Long Y, Zhang XL, Zhang XX, Hu HM, Li ZL, Hou FX, Ge F, Gao SB, Pan GT, Ma LL, Shen YO (2021) Genetic variations in *ZmSAUR15* contribute to the formation of immature embryo-derived embryonic calluses in maize. Plant J. 109(4):980-991. https://doi.org/10.1111/tpj.15609

Wu GY, Wei XL, Wang X, Wei Y (2020) Changes in biochemistry and histochemical characteristics during somatic

embryogenesis in *Ormosia henryi* prain. Plant Cell Tiss Organ Cult. 144:1-13. https://doi.org/10.1007/s11240-020-01973-5
Yue JH, Dong Y, Du CM, Shi YB, Teng Y (2022) Transcriptomic and physiological analyses reveal the acquisition of somatic embryogenesis potential in *Agapanthus praecox*. Sci Hortic. 305:111362. https://doi.org/10.1016/j.scienta.2022.111362
Zhang DP, Li ZY, Htwe MY, Shi P, Wei XK, Nie H, Nin JJ, Wu LH, Khan FS, Yu Q, Batool S, Wang Y (2024) Insights into the developmental trajectories of zygotic embryo, embryogenic callus and somatic embryo in coconut by single-cell transcriptomic analysis. Ind Crops Prod. 212:118338. https://doi.org/10.1016/j.indcrop.2024.118338
Zhou T,Yang XY, Guo K, Deng JW, Xu J, Gao WH, Lindsey K, Zhang XL (2016) ROS homeostasis regulates somatic embryogenesis via the regulation of auxin signaling in cotton. Mol Cell Proteomics. 15(6):2108-2124. https://doi.org/10.1074/mcp.M115.049338